

Freeze–thaw-induced embolism in *Pinus contorta*: centrifuge experiments validate the ‘thaw-expansion hypothesis’ but conflict with ultrasonic emission data

Stefan Mayr¹ and John S. Sperry²

¹Department of Botany, University of Innsbruck, Sternwartestr. 15, A-6020 Innsbruck, Austria; ²Biology Department, University of Utah, 257S 1400E Salt Lake City, UT, USA

Summary

Author for correspondence:

Stefan Mayr

Tel: 0043 512 507 5924

Email: stefan.mayr@uibk.ac.at

Received: 29 September 2009

Accepted: 5 November 2009

New Phytologist (2010) **185**: 1016–1024

doi: 10.1111/j.1469-8137.2009.03133.x

Key words: bubble expansion, centrifuge, freeze–thaw, ice, *Pinus*, ultrasonic acoustic emission, vulnerability to embolism, xylem temperature.

- The ‘thaw-expansion hypothesis’ postulates that xylem embolism is caused by the formation of gas bubbles on freezing and their expansion on thawing. We evaluated the hypothesis using centrifuge experiments and ultrasonic emission monitoring in *Pinus contorta*.
- Stem samples were exposed to freeze–thaw cycles at varying xylem pressure (P) in a centrifuge before the percentage loss of hydraulic conductivity (PLC) was measured. Ultrasonic acoustic emissions were registered on samples exposed to freeze–thaw cycles in a temperature chamber.
- Freeze–thaw exposure of samples spun at -3 MPa induced a PLC of 32% (one frost cycle) and 50% (two cycles). An increase in P to -0.5 MPa during freezing had no PLC effect, whereas increased P during thaw lowered PLC to 7%. Ultrasonic acoustic emissions were observed during freezing and thawing at -3 MPa, but not in air-dried or water-saturated samples. A decrease in minimum temperature caused additional ultrasonic acoustic emissions, but had no effect on PLC.
- The centrifuge experiments indicate that the ‘thaw-expansion hypothesis’ correctly describes the embolization process. Possible explanations for the increase in PLC on repeated frost cycles and for the ultrasonic acoustic emissions observed during freezing and with decreasing ice temperature are discussed.

Introduction

Ice formation in plant xylem blocks the transport of water and can, in consequence, cause drought stress and cavitation if the canopy is actively transpiring (Cochard *et al.*, 2000). In addition to this instantaneous restriction of water supply, frost events can also affect the plant water transport system in the long term. Freeze–thaw-induced embolism has been reported for many woody angiosperms (e.g. Cochard & Tyree, 1990; Just & Sauter, 1991; Sperry & Sullivan, 1992; Lo Gullo & Salleo, 1993; Sperry *et al.*, 1994; Lipp & Nilsson, 1997; Utsumi *et al.*, 1998; Lemoine *et al.*, 1999; Nardini *et al.*, 2000; Zhu *et al.*, 2001), as well as for conifers (e.g. Sperry & Sullivan, 1992; Sparks & Black, 2000; Feild & Brodrigg, 2001; Sparks *et al.*, 2001; Feild *et al.*, 2002; Mayr *et al.*, 2002, 2003a,b, 2007; Pittermann & Sperry, 2003, 2006; Mayr & Zublasing, 2009). It is an important

ecological factor in all regions in which subzero temperatures occur.

The ‘thaw-expansion hypothesis’ (also ‘bubble formation hypothesis’; e.g. Sucoff, 1969; Ewers, 1985; Lo Gullo & Salleo, 1993; Davis *et al.*, 1999; Lemoine *et al.*, 1999; Hacke & Sperry, 2001; Sperry & Robson, 2001; Tyree & Zimmermann, 2002; Pittermann & Sperry, 2003, 2006) postulates the following mechanism for freeze–thaw-related embolism: when the sap freezes, gas bubbles are formed in the conduits because air is insoluble in ice; on thawing, these bubbles will expand if the pressure of the surrounding sap becomes sufficiently negative to counter the bubble-collapsing force of surface tension (Pittermann & Sperry, 2006).

There are many indications that the mechanism of freeze–thaw-induced embolism indeed follows the ‘thaw-expansion hypothesis’. (1) Bubbles are formed within the ice on freezing. Sucoff (1969) and Robson *et al.* (1988)

observed a central series of bubbles in frozen tracheids, and Ewers (1985) reported that narrow conduits contained smaller air bubbles than wide conduits. (2) Freeze–thaw-induced embolism formation depends on the bubble size. Because larger elements contain larger amounts of dissolved gas, larger bubbles will be formed within the ice, and the risk of embolism should increase. Assuming that a series of bubbles is formed within elements, the bubble size depends on the amount of dissolved gas per conduit length and, in consequence, on the diameter of the conduit (e.g. Davis *et al.*, 1999; Sperry & Robson, 2001; Pittermann & Sperry, 2003, 2006). Accordingly, the vulnerability to freeze–thaw-induced embolism positively correlates with the conduit diameter. Wood with an average conduit diameter below 30 μm was found to be resistant to freeze–thaw-induced embolism at moderately negative sap pressure (Davis *et al.*, 1999; Sperry & Robson, 2001). Accordingly, conifers with small tracheids, as well as vessel-less angiosperms, were reported to be hardly susceptible to freeze–thaw-induced embolism (Hammel, 1967; Sucoff, 1969; Sperry & Sullivan, 1992; Sperry *et al.*, 1994; Davis *et al.*, 1999; Feild & Brodribb, 2001; Feild *et al.*, 2002), whereas ring-porous species are extremely vulnerable (Cochard & Tyree, 1990; Lo Gullo & Salleo, 1993; Sperry *et al.*, 1994; Nardini *et al.*, 2000). (3) Freeze–thaw-induced embolism formation depends on the pressure of the xylem sap. It has been demonstrated that freeze–thaw-induced conductivity losses increase with decreasing pressure (Sperry & Sullivan, 1992; Langan *et al.*, 1997; Davis *et al.*, 1999; Sperry & Robson, 2001; Mayr *et al.*, 2003a; Pittermann & Sperry, 2006). Thus, even conifers are vulnerable when the sap pressure is sufficiently negative to expand the small bubbles formed in their narrow tracheids (Pittermann & Sperry, 2006). Several field studies have demonstrated that embolism formation on freeze–thaw events is amplified by drought stress (e.g. Lemoine *et al.*, 1999; Sparks & Black, 2000; Sparks *et al.*, 2001; Mayr *et al.*, 2002, 2003b).

In contrast with the findings described above, there are several aspects which are potentially in contradiction with the ‘thaw-expansion hypothesis’. (1) Conductivity losses increase with the number of freeze–thaw events. This was demonstrated in field studies (Sperry *et al.*, 1994; Sparks & Black, 2000; Sparks *et al.*, 2001; Mayr *et al.*, 2003b), as well as in experiments based on hydraulic (Mayr *et al.*, 2003a) or cryo-scanning electron microscopy (cryo-SEM) and ultrasonic (Mayr *et al.*, 2007; Mayr & Zublasing, 2009) methods. It is unclear why conduits may escape embolism formation during the first frost cycle, but succumb during consecutive cycles, when the conditions and, in particular, the pressure, remain unchanged. (2) The widest conduits are not consistently the most vulnerable ones. Cryo-SEM analysis revealed that some, but not all, wide tracheids, as well as some small tracheids, in the xylem of

Picea abies were embolized after exposure to repeated freeze–thaw events (Mayr *et al.*, 2007). In addition, clusters of air-filled tracheids were observed adjacent to water-filled tracheids of greater diameter. Following the ‘thaw-expansion hypothesis’, the widest tracheids should seemingly embolize first. (3) Ultrasonic acoustic emissions (UAEs) are emitted on freezing. Several studies have demonstrated that UAEs occur during the freezing process in angiosperms as well as in conifers (Weiser & Wallner, 1988; Raschi *et al.*, 1989; Kikuta & Richter, 2003). In experiments with repeated freeze–thaw cycles (Mayr *et al.*, 2007; Mayr & Zublasing, 2009), UAEs start exactly with the onset of freezing in the xylem and cease on thawing. These patterns were observed in potted *Picea abies* trees and in excised shoots of several conifer species. The ultrasonic activity was found only in drought-stressed samples, but not in air-dried or water-saturated controls.

To fully test the ‘thaw-expansion hypothesis’, it would be necessary to distinguish between the effects of freezing and effects of thawing on embolism formation. Up to now, this has only been possible with ultrasonic emission measurements, but UAEs are difficult to interpret and are probably not linearly correlated with embolism (Mayr & Zublasing, 2009). Cryo-SEM analyses enable a mainly qualitative analysis of the effects of freezing but not of thawing. The hydraulic technique (Sperry *et al.*, 1988), which is a direct measure of conductivity losses caused by embolism, has only been used to quantify the cumulative effects of freezing and thawing.

In this study, we used a cooling centrifuge (Alder *et al.*, 1997; Davis *et al.*, 1999; Pittermann & Sperry, 2003, 2006) to expose xylem samples to freeze–thaw events whilst under negative sap pressure (xylem pressure, P). With this experimental set-up, it was possible to vary P during freezing and thawing, respectively, and thus to study the effect of both processes independently. We exposed samples to low P during the whole freeze–thaw event or during freezing or thawing phases only. In addition, effects of the minimum temperature and repeated freeze–thaw cycles were studied. Experiments were made on a conifer species as conifer xylem has a relatively simple composition, and many data on freeze–thaw-induced embolism in conifers are already available (see last section in paragraph four of the introduction). We used *Pinus contorta*, because this species exhibits relatively wide tracheids; therefore, effects on hydraulic conductivity could be expected even after one freeze–thaw cycle (Pittermann & Sperry, 2006). For comparison with previous ultrasonic studies on conifer species with smaller tracheids, we repeated the measurements of ultrasonic activity of air-dried, water-saturated and drought-stressed samples of *P. contorta* during exposure in a temperature chamber and analysed the qualitative parameters of UAE. Ultrasonic emission testing was also used to quantify the effects of a

stepwise decrease in minimum temperature and to analyse the vulnerability to drought-induced embolism.

This experimental approach was designed to separate freezing-related effects on embolism formation and ultrasonic activity from thawing effects. According to the 'thaw-expansion hypothesis', embolism formation and UAEs should be caused only during the thawing phase and only when the xylem pressure is sufficiently negative.

Materials and Methods

Plant material

Samples of *Pinus contorta* Dougl. ex Loudon (Pinaceae) were collected in the Uinta/Wasatch-Cache National Forest in northern Utah (40°3'N, 111°47'W) in April 2007 (centrifuge experiments) and March 2008 (ultrasonic emission experiments). Branches with a basal diameter up to 2 cm were cut from adult trees, wrapped in plastic bags and transported to the laboratory at the University of Utah. Branches were re-cut at the base at least three times (*c.* 2 cm each time) to release xylem tension gradually under water, and saturated (bottle with *c.* 20 cm water, samples covered with plastic bag) at 4°C for at least 24 h.

For centrifuge experiments, stem segments, free of side twigs and 142 mm in length (according to centrifuge rotor diameter, see Materials and Methods), were cut under water from saturated branches. The bark was left intact with the exception of the distal ends, where 2 cm of bark was removed to avoid clogging with resin. All samples were flushed at 0.1 MPa with distilled and filtered (0.22 µm) KCl solution (20 mM) for 10 min in both directions to remove native embolism.

For ultrasonic emission measurements, saturated branches were tightly wrapped in plastic bags and sent to the laboratory of the University of Innsbruck (Austria). There, all samples were re-cut under water and saturated for another 24 h at room temperature. After this, the branches were dehydrated on the bench until a *P* value between -2.6 and -3.1 MPa was reached. For all branches, *P* measurements were performed in intervals during dehydration on side twigs with a pressure chamber (Model 1000 Pressure Chamber, PMS Instrument Company Corvallis, OR). The side-branch *P* value was assumed to be similar to the main axis *P* value as transpiration was extremely low. When the desired *P* value was reached, at least three measurements were taken to calculate the mean *P* value, before stem sections *c.* 20 cm long and 1–2 cm in diameter, and free of side twigs, were cut from the middle section of the branches. Samples were tightly wrapped in Parafilm (Alcan, Montreal, QC, Canada) to avoid further water loss. In addition to drought-stressed branches, samples were prepared from water-saturated branches, as well as from stem segments completely dehydrated in an oven (80°C for 24 h).

Centrifuge experiments

Stem segments were exposed to different *P* values and temperature courses in a Sorvall RC5C centrifuge (Kendro Laboratory Products, Newton, CT) equipped with a special rotor, which allowed three stems to be spun simultaneously (e.g. Pittermann & Sperry, 2006). The temperature during freeze–thaw cycles in the centrifuge was controlled by the centrifuge refrigeration settings and by an external bath (model 1157; VWR Scientific, West Chester, PA) that circulated heat transfer fluid (type XLT; Polyscience, Niles, IL) through copper tubing lining the rotor chamber. To measure air temperatures within the rotor (every minute) and xylem temperatures (every 10 s), a small datalogger (HOBO; Onset Computer, Pocasset, MA, USA) was mounted on a holder positioned in the centre of the rotor, and its external sensor was fixed in the xylem of one sample.

The hydraulic conductivity (*K*) of the samples was determined to analyse the effects of different *P* values and temperature treatments: *K* values after flushing (*K*_{init}, see section on Plant material) and after centrifuge experiments were measured gravimetrically with a pressure head of 4–5 kPa using distilled and filtered (0.22 µm) KCl solution (20 mM). The percentage loss of conductivity (PLC) was calculated according to Eqn 1:

$$\text{PLC} = 100(1 - K/K_{\text{init}}) \quad \text{Eqn 1}$$

Centrifuge experiments were performed according to the following protocols:

- (1) After measurement of *K*_{init}, stems were spun at 11 560 rpm (inducing *P* of -3 MPa) for 10 min at 5°C and, after this, *K* was re-measured.
- (2) Then, the samples were again spun in the centrifuge whilst being exposed to a freeze–thaw cycle. In the standard experiment, the centrifuge and bath were set to -10°C for 50 min as soon as the spinning velocity corresponding to the desired *P* value (Alder *et al.*, 1997) was reached. After this time, the temperatures were set to +20°C for 25 min before the samples were taken out of the centrifuge. Samples were spun at -3 MPa during the whole freeze–thaw cycle, or at -3 MPa during freezing and -0.5 MPa during thawing or, vice versa, at -0.5 MPa during freezing and -3 MPa during thawing. Control samples were spun for 75 min at -3 MPa without freezing (50 min at 5°C, 25 min at 20°C) to exclude effects of the spinning time.
- (3) In additional experiments, samples were exposed to two consecutive freeze–thaw cycles at -3 MPa and to a lower minimum temperature. In the latter experiment, bath and centrifuge temperatures were decreased to -10°C during 50 min and to -25°C during the consecutive 40 min,

before temperatures were set to -10°C and 20°C in the following 10 and 25 min, respectively.

Ultrasonic emission measurements

Ultrasonic emission analysis was performed with a PCI-2-based system (PAC 125 18-bit A/D, 3 kHz–3 MHz PCI2) and 150 kHz resonance sensors (R15/C, 80–400 kHz) connected to a 20/40/60 dB preamplifier set to 40 dB (all components: Physical Acoustics, Wolfegg, Germany). The threshold was set to 45 dB and the peak definition time, hit definition time and hit lockout time were 200 μs , 400 μs and 2 μs , respectively. The registration and analysis of UAEs were performed with AEwin software (Mistras Holdings Corporation, Princeton, NJ), whereby the time, counts, amplitude and absolute energy of the hits were registered. At the upper side (opposite wood) of the stem samples, *c.* 4 cm² of the bark was removed and the xylem was covered with silicone grease to improve the acoustic coupling and prevent transpiration, before the sensors were attached with clamps. We used metal springs (coated with plastic material) to maintain constant coupling pressure. As stems were used, for which the contact area between the sensor and sample is unknown, the effective coupling pressure could neither be adjusted nor determined.

Ultrasonic emission experiments were performed according to the following protocols:

- (1) Samples at a P value of *c.* -3 MPa, as well as air-dried and water-saturated samples (see Materials and Methods), were exposed to five freeze–thaw cycles in a cold–heat test chamber (MK53, Binder; for details see Mayr & Zublasing, 2009) according to the experimental protocol and temperature courses reported in Mayr *et al.* (2007). The chamber temperature was decreased from $+6^{\circ}\text{C}$ to -8°C within 1 h, kept at -8°C for 1 h, increased to $+6^{\circ}\text{C}$ within 1 h, and kept at $+6^{\circ}\text{C}$ for 1 h. Then, the next 4-h cycle started. Xylem temperature was measured in 1 min intervals with a thermocouple inserted into at least two samples, and stored by a data logger (CR10X, Campbell Scientific, Loughborough, Leicestershire, UK).
- (2) Samples at a P value of *c.* -3 MPa were exposed to one freeze–thaw cycle, whereby the chamber temperature was decreased stepwise to -8°C , -16°C and -32°C in 3 h intervals, before being increased to 0°C during the consecutive 4 h.
- (3) The ultrasonic system was also used to analyse the vulnerability to drought-induced embolism. R15 sensors were attached to the main stem of saturated branches before they were dehydrated on the bench. In intervals, the P values of the side twigs were measured (Scholander technique, see Plant material section). The cumulative number of UAEs corresponding to the measured P value was related to the total number of UAEs until complete dehydration. Vulner-

ability curves for branches dehydrated to various extents were obtained by plotting UAE (%) vs P . Curves were fitted with an exponential sigmoidal equation (Pammenter & Vander Willigen, 1998):

$$\text{cumulative UAE} = 100 / (1 + \exp(a(P - P_{50}))) \quad \text{Eqn 2}$$

where the cumulative UAE is in per cent, P is the corresponding xylem pressure and parameter a is related to the slope of the curve. P_{50} corresponds to P at 50% of total UAE. The vulnerability curve was calculated using Fig.P 2.98 (Biosoft Corporation, Cambridge, UK).

Number of samples and statistics

In centrifuge experiments, eight samples were used in the standard temperature treatment (control: five samples), and six samples for experiments with a minimum temperature of -25°C and two freeze–thaw cycles. Ultrasonic emission measurements were performed on 28 samples at -3 MPa and on 10 water-saturated and eight air-dried samples. Eight samples (-3 MPa) were exposed to a freezing cycle with a minimum temperature of -32°C . For vulnerability analysis, eight branches were dehydrated and 62 ψ measurements were taken.

The results of hydraulic measurements and UAE quality parameters are given as mean \pm SE. Differences were tested with Student's t -test after testing for the Gaussian distribution (Kolmogorov–Smirnov test) and variance homogeneity (Levene test) of the data. In the case of inhomogeneous variances, the Tamhane test was used. For data not distributed normally, differences were tested using the Mann–Whitney U -test. All tests were performed pairwise at a probability level of 5% using SPSS (Ver. 15.0; SPSS Inc., Chicago, IL).

Results

Vulnerability to drought-induced embolism

Vulnerability analysis based on the ultrasonic method worked very well with *P. contorta*. Its P_{50} value was -3.42 ± 0.05 MPa and parameter a (corresponding to the slope of the vulnerability curve) was 2.78 ± 0.37 . Figure 1 also demonstrates that samples spun at -3 MPa or dehydrated to *c.* -3 MPa were close to the upper threshold of drought-induced embolism.

Centrifuge experiments

Temperature measurements revealed that the air temperatures within the rotor fluctuated as a result of the cooling regulation of the centrifuge (Fig. 2). However, xylem temperatures showed a continuous course with maximum rates during cooling and warming of 1.6 and 1.2 K min⁻¹,

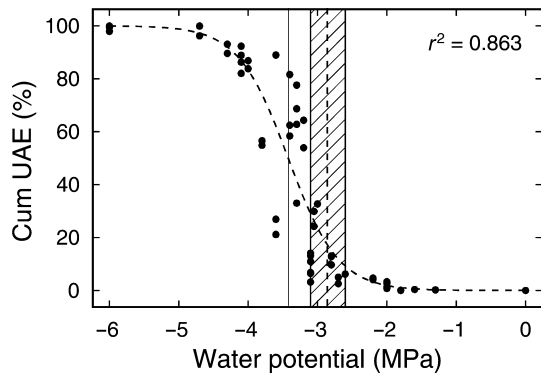


Fig. 1 Vulnerability to drought-induced embolism in *Pinus contorta*. The relative number of cumulative acoustic events was plotted vs xylem pressure and fitted with an exponential sigmoidal equation (Pammenter & Vander Willigen, 1998). Full vertical line, pressure at 50% loss of xylem conductivity; broken line and hatched area, mean, lowest and highest xylem pressure of samples used in ultrasonic experiments.

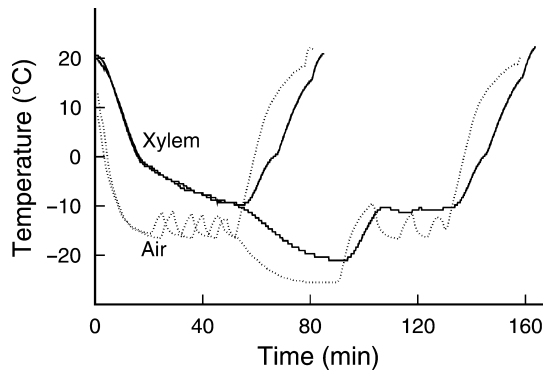


Fig. 2 Temperature courses during centrifuge experiments in *Pinus contorta*. Dotted line, air temperatures within the rotor; full line, xylem temperatures during spinning at a xylem pressure of -3 MPa. Courses for experiments with minimum temperatures of -15°C and -25°C are given.

respectively. When centrifuge and bath temperatures were set to -15°C and -25°C , minimum air temperatures within the rotor were -16.6°C and -25.5°C and minimum xylem temperatures were -9.8°C and -21.1°C , respectively.

Spinning of stems at a P value of -3 MPa without any freeze–thaw cycle caused only low PLC ($4.4 \pm 1.2\%$). The PLC at this P value did not differ when the samples were spun for 10 min or for the 85 min period used in the freeze–thaw experiments (Fig. 3). By contrast, a freeze–thaw cycle at -3 MPa caused an increase in PLC to $32.2 \pm 4.0\%$. A nearly identical PLC was also observed when samples were exposed to -3 MPa during thawing and to -0.5 MPa during freezing ($35.2 \pm 4.3\%$). By contrast, PLC was only $6.7 \pm 1.9\%$ when the P value was -3 MPa during freezing but -0.5 MPa during thawing (Fig. 3).

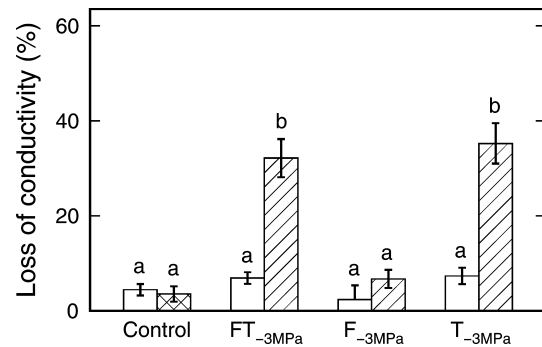


Fig. 3 Effects of xylem pressure during freezing and thawing on hydraulic conductivity in *Pinus contorta*. Bars indicate the loss of conductivity after 10 min of spinning at 5°C and -3 MPa (open), or after an additional 75 min exposure to one freeze–thaw cycle with different xylem pressure treatments (hatched). Samples were spun at -3 MPa during the whole freeze–thaw cycle ($\text{FT}_{-3\text{MPa}}$), at -3 MPa during freezing and -0.5 MPa during thawing ($\text{F}_{-3\text{MPa}}$) or at -0.5 MPa during freezing and -3 MPa during thawing ($\text{T}_{-3\text{MPa}}$). Control samples were spun at -3 MPa for 10 and 75 min (cross-hatched bar) without freezing to test the effect of the spinning time. Mean \pm SE. Bars not followed by the same letter differ significantly at $P \leq 0.05$.

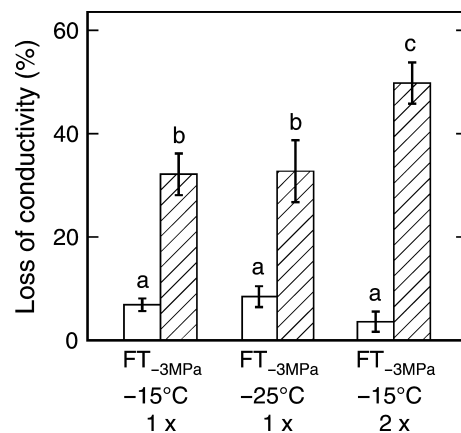


Fig. 4 Effects of temperature courses on hydraulic conductivity in *Pinus contorta*. Bars indicate the loss of conductivity after 10 min of spinning at 5°C and -3 MPa (open) or after additional freeze–thaw treatment (hatched). Samples were exposed to one freezing cycle with a minimum air temperature of -25°C (second hatched column) or to two freeze–thaw cycles at -15°C (third hatched column). The first column shows the results of the standard experiment with one freeze–thaw cycle at -15°C (identical to $\text{FT}_{-3\text{MPa}}$ in Fig. 3). Mean \pm SE. Bars not followed by the same letter differ significantly at $P \leq 0.05$.

No significant effect of the minimum temperature on PLC was observed in centrifuge experiments (Fig. 4). After one freeze–thaw cycle with a stepwise decrease in the xylem temperature to $c. -21^{\circ}\text{C}$ (Fig. 2), PLC was $32.7 \pm 6.0\%$, and thus similar to the PLC after the standard temperature treatment. When stems were exposed to two consecutive freeze–thaw events instead of one, PLC increased significantly to $49.8 \pm 4.0\%$.

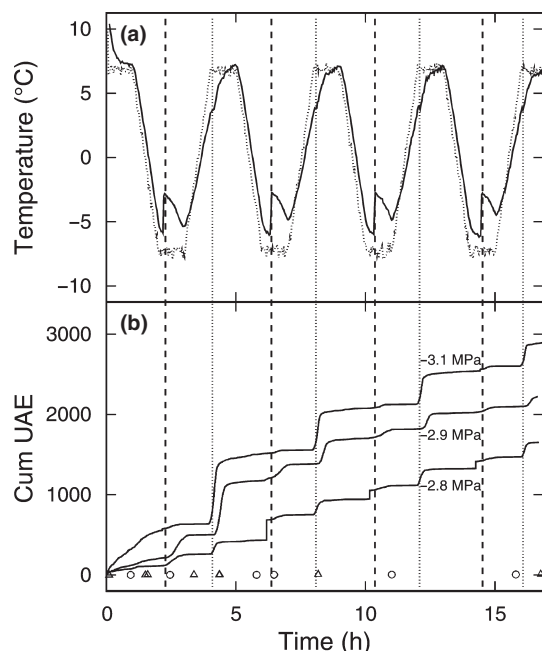


Fig. 5 Ultrasonic acoustic emissions during freeze–thaw cycles. *Pinus contorta* stem samples were exposed to five consecutive freeze–thaw cycles in a test chamber. The chamber air temperature (dotted line) and xylem temperature (full line) are given in (a). (b) The course of the cumulative number of acoustic events (cum UAE) of three samples dehydrated to a xylem pressure near -3 MPa (full lines) and of water-saturated (circles) or air-dried (triangles) samples. Vertical lines indicate the onset of freezing (broken) and thawing (dotted).

Ultrasonic emission measurements in freeze–thaw experiments

All stems frozen and thawed at a P value of $c. -3$ MPa showed high ultrasonic activities. In Fig. 5, three typical courses of cumulative UAE are given. The absolute number of UAEs between samples differed, ranging from 81 to 6385, which was probably a result of unavoidable variation in acoustic coupling (see Materials and Methods, and Mayr & Zublasung, 2009). However, the pattern of UAE courses was similar in all -3 MPa samples: ultrasonic activity was observed during freezing and during thawing, whereby the onset corresponded exactly with the freezing exotherm and the thawing endotherm (Fig. 5). In most cases, thawing caused more UAE than freezing. In contrast with the -3 MPa samples, air-dried and water-saturated samples showed very low ultrasonic activity. Xylem cooling and thawing rates in these experiments were 0.22 and 0.17 K min^{-1} , respectively.

A stepwise cooling to -8 , -16 and -32°C caused UAE during all cooling periods (Fig. 6). Ultrasonic activity was highest during cooling to -8°C , whereas the increase in cumulative UAE during consecutive cooling steps became less and less pronounced. Some acoustic activity was also observed when the warming process started.

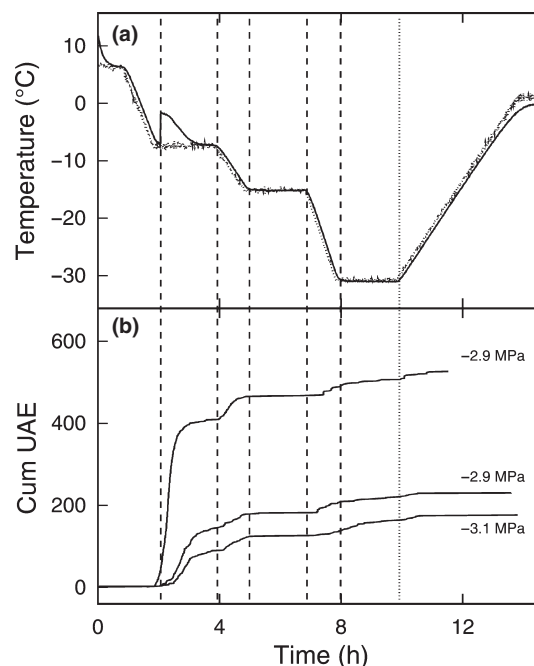


Fig. 6 Ultrasonic acoustic emissions during cooling to -32°C . *Pinus contorta* stem samples were exposed to one freeze–thaw cycle in a test chamber, which was stepwise cooled to -8 , -16 and -32°C before being warmed to 0°C . The chamber air temperature (dotted line) and xylem temperature (full line) are given in (a). (b) The course of the cumulative number of acoustic events (cum UAE) of three samples dehydrated to a xylem pressure near -3 MPa (full lines). Vertical lines indicate the onset of freezing and consecutive temperature decreases (broken), as well as the start of the temperature increase (dotted).

A comparison of the signal characteristics of UAE on freezing, thawing (in -3 MPa samples) and dehydration (Table 1) revealed, because of the large number of samples, significant differences between all groups. Nevertheless, differences in amplitude and absolute energy between UAE on freezing and on thawing were too small to indicate any relevance. These signals might only differ in the number of counts (peaks of the acoustic waves). The amplitudes and counts of drought-induced UAE (mean of all signals emitted during dehydration) were similar to freeze–thaw-induced signals, but the absolute energy was considerably lower.

Discussion

Pinus contorta was resistant to drought-induced embolism down to a P value of $c. -3$ MPa. The vulnerability analysis based on the ultrasonic method (Fig. 1) revealed a P_{50} value of -3.42 ± 0.05 MPa, which is similar to that of hydraulic measurements on material from the same *P. contorta* stand (-3.7 MPa; Pittermann & Sperry, 2006). In our experiments, samples were spun at -3 MPa or dehydrated to $c. -3$ MPa, because previous studies have indicated that the

Table 1 Characteristics of ultrasonic signals

	Counts (number per hit)	Amplitude (dB)	Absolute energy (aJ)	<i>n</i>
Freezing	3.31 ± 0.02 ^a	48.8 ± 0.02 ^a	131.4 ± 3.1 ^a	22 101
Thawing	3.49 ± 0.02 ^b	49.1 ± 0.02 ^b	131.4 ± 1.5 ^b	35 027
Dehydration	3.37 ± 0.01 ^c	48.61 ± 0.01 ^c	117.4 ± 0.3 ^c	2 060 211

Counts (number of peaks of the acoustic wave), amplitude and absolute energy of ultrasonic acoustic emissions induced by freezing, thawing or dehydration in *Pinus contorta*. The last column gives the number (*n*) of signals analysed (number of signals registered during freezing, thawing or dehydration and cumulated for all samples). Mean ± SE. Values not followed by the same letter differ significantly at $P \leq 0.05$.

effect of freeze–thaw stress is highest near the upper drought-induced vulnerability threshold (Mayr *et al.*, 2003a, 2007; Pittermann & Sperry, 2006; Mayr & Zublas-ing, 2009). The cooling and thawing rates used in ultrasonic emission experiments were *c.* 0.2 K min⁻¹, and thus similar to those of previous studies (Pittermann & Sperry, 2003; Mayr *et al.*, 2007; Mayr & Zublas-ing, 2009). To save time, higher temperature rates were chosen in centrifuge experiments (*c.* 1.4 K min⁻¹). The effects of freeze–thaw treatment at these rates (see next paragraph) were similar to the effects reported in Pittermann & Sperry (2006), who performed experiments at 0.2 K min⁻¹. We conclude that the variation in temperature rates between 0.2 and 1.6 K min⁻¹ did not influence substantially embolism formation.

Centrifuge experiments

The main centrifuge experiments of our study clearly supported the ‘thaw-expansion hypothesis’. One freeze–thaw event at a spinning velocity corresponding to a *P* value of -3 MPa caused a 27.8% increase in PLC compared with the effect of exposure to -3 MPa only (Fig. 3). Pittermann & Sperry (2006) reported a similar PLC (*c.* 35%). In this and the present study, control experiments proved that the duration of spinning by itself had no significant effect on the extent of embolism (Fig. 3). When the *P* value was held at -3 MPa only during thawing, but at -0.5 MPa during freezing ($T_{-3 \text{ MPa}}$ in Fig. 3), a similar PLC was observed (30.8%). By contrast, no significant embolism was found when the *P* value was held at -3 MPa during freezing and at -0.5 MPa during thawing ($F_{-3 \text{ MPa}}$ in Fig. 3). This confirms that it is *P* during thawing that is critical for the formation of freeze–thaw-induced embolism. As predicted by the ‘thaw-expansion hypothesis’, the expansion of bubbles during thawing depends on a sufficiently negative *P* value, whereas bubble formation during freezing is not influenced by *P*.

It was also in accordance with the ‘thaw-expansion hypothesis’ that no effect of the minimum temperature was observed, as bubbles should be formed regardless of ice temperature (Langan *et al.*, 1997). Figure 4 demonstrates that a further 10 K temperature decrease after the first freezing step caused no increase in PLC compared

with the standard temperature treatment. In addition, Pittermann & Sperry (2003) found no effect on embolism formation in *P. contorta* when the minimum temperature was varied. By contrast, an increasing PLC on lower minimum temperature, perhaps caused by damage to parenchyma tissues, was observed in *Ginkgo biloba* (Pittermann & Sperry, 2003) and *Larrea tridentata* (Pockman & Sperry, 1997).

One of our centrifuge results was ambiguous with respect to the ‘thaw-expansion hypothesis’. Exposure of stems to two consecutive temperature cycles (minimum xylem temperature *c.* -10°C) increased PLC significantly by another 17.6% compared with one freeze–thaw treatment. In other words, one-third of tracheids embolized after two temperature cycles were still functional after the first freeze–thaw event. We can provide two possible explanations for this phenomenon. First, Pittermann & Sperry (2003) have already suggested that ‘a certain degree of stochasticity’ should influence embolism formation. By chance, there will be considerable variation in bubble size even within tracheids of the same diameter. Bubble size can be further influenced by freezing and thawing rates (Robson & Petty, 1987; Robson *et al.*, 1988; Sperry & Robson, 2001). To estimate the variability of bubble formation during thawing, deeper insights into the spatial and temporal dynamics of ice formation in the xylem would be necessary. Second, Sucoff (1969) have postulated that the expansion of the largest population of bubbles during a thaw should cause an increase in *P* in adjacent conduits via the redistribution of water, which would suppress embolism formation in the latter elements. Consequently, another portion of conduits could embolize with each cycle. Améglio *et al.* (2001) reported extensive water shifts between wood and bark during freeze–thaw events, and Mayr *et al.* (2007) found indications that water might be irreversibly trapped in extracellular spaces. This could also lead to a stepwise embolization during consecutive freeze–thaw cycles.

Ultrasonic emission experiments

In the presented experiments, UAEs were observed only in samples at a xylem pressure of -3 MPa, whereas negligible ultrasonic activity was found in water-saturated and air-dried

samples. This is similar to the patterns shown for several other conifers, but, in contrast with previous ultrasonic emission studies (Mayr *et al.*, 2007; Mayr & Zublasing, 2009), which reported UAEs exclusively during freezing, UAEs were registered during freezing and thawing (Fig. 5). The onset of ultrasonic activity thereby clearly corresponds to the start of the freezing or thawing processes indicated by the temperature exotherms and endotherms. We suggest that UAEs registered during thawing correspond to embolism formation according to the 'thaw-expansion hypothesis'. Consistent with this is the concordant increase in PLC and cumulative thaw UAEs during repeated freeze-thaw cycles. UAEs on thawing were probably detected only in *P. contorta* because only its tracheids are wide enough to be susceptible to the mechanism. In the other conifers (Mayr *et al.*, 2007; Mayr & Zublasing, 2009), the tracheids are too small to cause the formation of bubbles which expand during thawing based on the data from Pittermann & Sperry (2003).

UAEs observed on freezing were probably not related to the mechanism postulated by the 'thaw-expansion hypothesis': UAEs from cavitating xylem are related to the release of energy stored in the cell walls on low P (Tyree & Sperry, 1989) and, accordingly, freezing caused UAEs only in samples at -3 MPa but not in water-saturated samples (Fig. 5). Thus, freezing-associated UAE requires low P (whereas embolism formation according to the 'thaw-expansion hypothesis' does not; see above), which indicates an independent underlying process (Mayr & Zublasing, 2009; also see Kikuta & Richter, 2003).

If the freezing-associated UAE is also caused by cavitation and embolism, the embolism was too subtle to be detected by PLC techniques. Cavitation during the freezing phase could occur in several ways. The outgassed bubbles could expand if the surrounding liquid sap is under negative P . However, the expansion of ice would tend to pressurize the unfrozen sap, and transpiration rates during the freezing phase were negligible under the experimental conditions. Alternatively, the extremely low water potential of ice could potentially create severe negative P in the unfrozen sap and cause cavitation by air seeding from adjacent, already air-filled spaces (Mayr *et al.*, 2007; Mayr & Zublasing, 2009). Sparks *et al.* (2001) suggested that the low water potential of ice was responsible for embolism formation in *P. contorta*. It is unclear which of these contrasting effects, pressurization as a result of ice expansion or low water potential of ice, prevails, and whether complex and dynamic changes in P might occur during the freezing process. As a result of the rapid movement of the ice front through the xylem, embolization may be restricted to only a few tracheids during each freezing event (Mayr *et al.*, 2007). However, such a mechanism is difficult to reconcile with the continued production of UAEs as the ice temperature drops (Fig. 6). For the latter effect, one would have to postulate that the sap in a few

tracheids remains liquid even when most of the xylem is frozen. The UAEs could not originate from tracheid cavitation if the tracheids were already frozen.

The lack of concordance between PLC data and the freezing-phase UAEs could also suggest that these UAEs may not originate from tracheid cavitation during freezing. Instead, these UAEs may originate from some other source of mechanical stress. Ristic & Ashworth (1993) reported protoplast fragmentation and ultrastructural damage in xylem ray parenchyma on freezing, and that symplast cavitation could potentially create UAEs. Continued UAE production with decreasing ice temperature (and hence ice water potential) may reflect continued stresses arising from the redistribution of tissue water. Importantly, however, the water-saturated controls showed little or no UAE activity, yet they were exposed to the same desiccating and expanding forces of ice (Fig. 6).

Clearly, much more research is required to understand the cause of freezing-associated UAEs, and a deeper analysis of qualitative UAE parameters, such as UAE energy (Rosner *et al.*, 2006), might be helpful. We observed no relevant difference in the characteristics of UAE signals on freezing vs thawing, whereas the energy of drought-induced UAEs was lower overall (Table 1). This was also the case when only signals emitted at $c. -3$ MPa were considered (data not shown). Knowledge on the quality of UAEs derived from xylem is poor (also see Mayr & Zublasing, 2009), so that we do not yet know whether different UAE qualities might reflect differences in the underlying embolization processes.

Conclusion

There is evidence that the 'thaw-expansion hypothesis' correctly describes the process of embolization by bubble expansion during thawing. UAE production during freezing or afterwards with lowered ice temperature was not associated with a measurable increase in PLC in *P. contorta*. Our results were inconclusive with regard to the origin of freezing-associated UAEs in conifer xylem. It remains to be analysed whether these UAEs are related to the formation of xylem embolism or other processes during freezing. A better knowledge of the dynamics and spatial patterns of ice formation and propagation in the xylem might be the key to explain the observed freezing effects, as well as the increase in embolism on repeated frost cycles.

Acknowledgements

This study was supported by APART (Austrian Programme for Advanced Research and Technology) and FWF ('Fonds zur Förderung der Wissenschaftlichen Forschung'). We thank Maggie Caird Christman for helpful assistance.

References

- Alder NN, Pockman WT, Sperry JS, Nuismer S. 1997. Use of centrifugal force in the study of xylem cavitation. *Journal of Experimental Botany* **48**: 665–674.
- Améglio T, Cochard H, Ewers FW. 2001. Stem diameter variations and cold hardiness in walnut trees. *Journal of Experimental Botany* **52**: 2135–2142.
- Cochard H, Tyree MT. 1990. Xylem dysfunction in *Quercus*: vessel sizes, tyloses, cavitation and seasonal changes in embolism. *Tree Physiology* **6**: 393–407.
- Cochard H, Bodet C, Améglio T, Cruiziat P. 2000. Cryo-scanning electron microscopy observations of vessel content during transpiration in walnut petioles. Facts or artifacts?. *Plant Physiology* **124**: 1191–1202.
- Davis SD, Sperry JS, Hacke UG. 1999. The relationship between xylem conduit diameter and cavitation caused by freezing. *American Journal of Botany* **86**: 1367–1372.
- Ewers FW. 1985. Xylem structure and water conduction in conifer trees, dicot trees and lianas. *International Association of Wood Anatomy Bulletin* **6**: 309–317.
- Feild TS, Brodribb T. 2001. Stem water transport and freeze–thaw xylem embolism in conifers and angiosperms in a Tasmanian treeline heath. *Oecologia* **127**: 314–320.
- Feild TS, Brodribb T, Holbrook NM. 2002. Hardly a relict: freezing and the evolution of vesselless wood in Winteraceae. *Evolution* **56**: 464–478.
- Hacke UG, Sperry JS. 2001. Functional and ecological xylem anatomy. *Perspectives in Plant Ecology, Evolution and Systematics* **4**: 97–115.
- Hammel HT. 1967. Freezing of xylem sap without cavitation. *Plant Physiology* **42**: 55–66.
- Just J, Sauter JJ. 1991. Changes in hydraulic conductivity upon freezing of the xylem of *Populus × canadensis* Moench “robusta”. *Trees* **5**: 117–121.
- Kikuta SB, Richter H. 2003. Ultrasound acoustic emissions from freezing xylem. *Plant, Cell & Environment* **26**: 383–388.
- Langan SJ, Ewers FW, Davis SD. 1997. Xylem dysfunction caused by water stress and freezing in two species of co-occurring chaparral shrubs. *Plant, Cell & Environment* **20**: 425–437.
- Lemoine D, Granier A, Cochard H. 1999. Mechanism of freeze-induced embolism in *Fagus sylvatica* L. *Trees* **13**: 206–210.
- Lipp CC, Nilsen ET. 1997. The impact of subcanopy light environment on the hydraulic vulnerability of *Rhododendron maximum* to freeze–thaw cycles and drought. *Plant, Cell & Environment* **20**: 1264–1272.
- Lo Gullo MA, Salleo S. 1993. Different vulnerabilities of *Quercus ilex* L. to freeze- and summer drought-induced xylem embolism: an ecological interpretation. *Plant, Cell & Environment* **16**: 511–519.
- Mayr S, Zublasing V. 2009. Ultrasonic emissions from conifer xylem exposed to repeated freezing. *Journal of Plant Physiology* **167**: 34–40.
- Mayr S, Wolfschwenger M, Bauer H. 2002. Winter-drought induced embolism in Norway spruce (*Picea abies*) at the Alpine timberline. *Physiologia Plantarum* **115**: 74–80.
- Mayr S, Gruber A, Bauer H. 2003a. Repeated freeze–thaw cycles induce embolism in drought stressed conifers (Norway spruce, stone pine). *Planta* **217**: 436–441.
- Mayr S, Schwienbacher F, Bauer H. 2003b. Winter at the Alpine timberline: why does embolism occur in Norway spruce but not in stone pine? *Plant Physiology* **131**: 780–792.
- Mayr S, Cochard H, Améglio T, Kikuta S. 2007. Embolism formation during freezing in the wood of *Picea abies*. *Plant Physiology* **143**: 60–67.
- Nardini A, Salleo S, Lo Gullo MA, Pitt F. 2000. Different responses to drought and freeze stress of *Quercus ilex* L. growing along a latitudinal gradient. *Plant Ecology* **148**: 139–147.
- Pammenter NW, Vander Willigen C. 1998. A mathematical and statistical analysis of the curves illustrating vulnerability of xylem to cavitation. *Tree Physiology* **18**: 589–593.
- Pittermann J, Sperry JS. 2003. Tracheid diameter is the key trait determining the extent of freezing-induced embolism in conifers. *Tree Physiology* **23**: 907–914.
- Pittermann J, Sperry JS. 2006. Analysis of freeze–thaw embolism in conifers. The interaction between cavitation pressure and tracheid size. *Plant Physiology* **140**: 374–382.
- Pockman WT, Sperry JS. 1997. Freezing-induced xylem cavitation and the northern limit of *Larrea tridentata*. *Oecologia* **109**: 19–27.
- Raschi A, Scarascia Mugnozza G, Surace R, Valentini R, Vazzana C. 1989. The use of ultrasound technique to monitor freezing and thawing of water in plants. *Agriculture, Ecosystems and Environment* **27**: 411–418.
- Ristic Z, Ashworth EN. 1993. Ultrastructural evidence that intracellular ice formation and possibly cavitation are the sources of freezing injury in supercooling wood tissue of *Cornus florida* L. *Plant Physiology* **103**: 753–761.
- Robson DJ, Petty JA. 1987. Freezing in conifer xylem I. Pressure changes and growth velocity of ice. *Journal of Experimental Botany* **38**: 1901–1908.
- Robson DJ, McHardy WJ, Petty JA. 1988. Freezing in conifer xylem II. Pit aspiration and bubble formation. *Journal of Experimental Botany* **39**: 1617–1621.
- Rosner S, Klein A, Wimmer R, Karlsson B. 2006. Extraction of features from ultrasound acoustic emissions: a tool to assess the hydraulic vulnerability of Norway spruce trunkwood? *New Phytologist* **171**: 105–116.
- Sparks JP, Black RA. 2000. Winter hydraulic conductivity and xylem cavitation in coniferous trees from upper and lower treeline. *Arctic, Antarctic and Alpine Research* **32**: 397–403.
- Sparks JP, Campbell GS, Black RA. 2001. Water content, hydraulic conductivity, and ice formation in winter stems of *Pinus contorta*: a TDR case study. *Oecologia* **127**: 468–475.
- Sperry JS, Robson DJ. 2001. Xylem cavitation and freezing in conifers. In: Bigras FJ, Colombo SJ, eds. *Conifer cold hardiness*. Dordrecht, the Netherlands: Kluwer Academic Publishers, 121–136.
- Sperry JS, Sullivan JEM. 1992. Xylem embolism in response to freeze–thaw cycles and water stress in ring-porous, diffuse-porous and conifer species. *Plant Physiology* **100**: 605–613.
- Sperry JS, Donnelly JR, Tyree MT. 1988. A method for measuring hydraulic conductivity and embolism in xylem. *Plant, Cell & Environment* **11**: 35–40.
- Sperry JS, Nichols KL, Sullivan JEM, Eastlack SE. 1994. Xylem embolism in ring-porous, diffuse-porous, and coniferous trees of northern Utah and interior Alaska. *Ecology* **75**: 1736–1752.
- Suocoff E. 1969. Freezing of conifer xylem and the cohesion–tension theory. *Physiologia Plantarum* **22**: 424–431.
- Tyree MT, Sperry JS. 1989. Characterization and propagation of acoustic emission signals in woody plants: towards an improved acoustic emission counter. *Plant, Cell & Environment* **12**: 371–382.
- Tyree MT, Zimmermann MH. 2002. *Xylem structure and the ascent of sap*. Berlin, Germany: Springer Verlag.
- Utsumi Y, Sano Y, Fujikawa S, Funada R, Ohtani J. 1998. Visualization of cavitated vessels in winter and refilled vessels in spring in diffuse-porous trees by cryo-scanning electron microscopy. *Plant Physiology* **117**: 1463–1471.
- Weiser RL, Wallner SJ. 1988. Freezing woody plant stems produces acoustic emissions. *Journal of the American Society for Horticultural Science* **113**: 636–639.
- Zhu XB, Cox RM, Meng FR, Arp PA. 2001. Responses of xylem cavitation, freezing injury and shoot dieback to a simulated winter thaw in yellow birch seedlings growing in different nursery culture regimes. *Forest Ecology and Management* **145**: 243–253.